IJP (2026), Vol. 13, Issue 8 **(Research Article)**

Received on 22 June 2026; received in revised form, 15 July 2026; accepted, 23 July 2026; published 01 August 2026

NANOFORMULATION OF CURCUMIN AND ITS ANTI-INFLAMMATORY EVALUATION

Y. P. Karade, R. N. Kausdikar * and M. J. Patil

Department of Pharmacognosy, ASPM College of Pharmacy, Vaibhavwadi, Sindhdurg - 416810, Maharashtra, India.

Keywords:

Curcumin, Chitosan nanoparticles, Anti inflammatory, Nanoformulation

Correspondence to Author:
Dr. Rajashri N. Kausdikar

Associate Professor,
Department of Pharmacognosy,
ASPM College of Pharmacy,
Vaibhavwadi, Sindhdurg - 416810,
Maharashtra, India.

E-mail: researchaspm@gmail.com

ABSTRACT: Curcumin, the principal polyphenolic constituent of Curcuma longa (turmeric), possesses potent anti-inflammatory activity. Despite remarkable pharmacological potential, clinical translation of curcumin is severely restricted by its drawbacks. The present study aimed to develop, optimize, and evaluate curcumin-loaded chitosan nanoparticles using Box-Behnken Design (BBD), and to compare their *in-vitro* antiinflammatory activity with free curcumin and the reference. Curcumin was extracted from dried *Curcuma longa* rhizomes and purified by silica gel column chromatography. An HPLC-UV analytical method was developed and fully validated per ICH Q2(R1) guidelines. The optimized formulation was characterized by dynamic light scattering (DLS), TEM, SEM, FTIR, DSC, and XRPD. *In-vitro* drug release, antiinflammatory activity and stability studies were conducted. Extracted curcumin showed 98.6% HPLC purity and confirmed identity by UV, FTIR, and melting point. BBD optimization yielded an optimal formulation with particle size 186.4 ± 7.8 nm, PDI 0.194 ± 0.018, zeta potential +28.6 ± 2.4 mV, and encapsulation efficiency 87.2 ± 1.6%. Solid-state characterization confirmed amorphous dispersion of curcumin within the chitosan matrix. Drug release followed 84.6% cumulative release over 72 hours. Curcumin nanoparticles demonstrated 3.8-fold superior anti-inflammatory potency versus free curcumin in both albumin denaturation inhibition (IC50: 44.6 vs. 168.4 µg/mL) and HRBC membrane stabilization (IC50: 48.2 vs. 184.6 µg/mL) assays, with potency comparable to diclofenac sodium. Nanoencapsulated curcumin showed 46-fold superior chemical stability versus free curcumin under accelerated conditions. The nanoformulation represents a promising, pharmaceutically validated platform for improving the therapeutic utility of curcumin as a safe and effective natural anti-inflammatory agent.

INTRODUCTION: Curcumin (1,7-bis(4-hydroxy-3-methoxyphenyl)-1,6-heptadiene-3,5-dione), the principal bioactive polyphenolic compound isolated from the rhizomes of *Curcuma longa* Linn. (Family Zingiberaceae), commonly known as turmeric, represents one of the most thoroughly investigated natural therapeutic agents in contemporary biomedical science.

QUICK RESPONSE CODE

DOI: 10.13040/IJPSR.0975-8232.IJP.13(8).812-28

Article can be accessed online on: www.ijpjournal.com

DOI link: https://doi.org/10.13040/IJPSR.0975-8232.IJP.13(8).812-28

Its vibrant yellow-orange pigmentation, which has rendered turmeric indispensable in culinary, cosmetic, and cultural traditions across the Indian subcontinent and Southeast Asia for more than four thousand years, belies a remarkably complex pharmacological profile that continues to attract intensive scientific scrutiny worldwide.

The compound belongs to the curcuminoid class of natural polyphenols, which also includes demethoxycurcumin and bisdemethoxycurcumin; curcumin itself constitutes approximately 77% of the total curcuminoid content of commercial turmeric extract and is principally responsible for the pharmacological activity attributed to the whole

extract [1]. Inflammation is a fundamental biological response involved in the pathogenesis of numerous chronic diseases, including rheumatoid arthritis, inflammatory bowel disease, cardiovascular disorders, diabetes mellitus, neurodegenerative diseases, and cancer. Although conventional anti-inflammatory drugs such as non-steroidal anti-inflammatory drugs (NSAIDs) and corticosteroids are widely used, their long-term administration is frequently associated with serious adverse effects including gastrointestinal ulceration, nephrotoxicity, hepatotoxicity, immuno-suppression, and cardiovascular complications. Therefore, there is a continuing need for safer and more effective anti-inflammatory agents [2, 3].

Curcumin, the principal bioactive constituent of *Curcuma longa* (turmeric), possesses well-documented anti-inflammatory, antioxidant, and immunomodulatory activities. It exerts its pharmacological effects through the modulation of multiple inflammatory pathways including NF-κB, COX-2, LOX, TNF-α, IL-1β, and IL-6. Despite its remarkable therapeutic potential, the clinical application of curcumin is severely limited by its poor aqueous solubility, low gastrointestinal absorption, rapid metabolism, chemical instability, and extremely low oral bioavailability [4, 5].

Nanotechnology-based drug delivery systems have emerged as a promising strategy to overcome these limitations. Polymeric nanoparticles prepared using biodegradable and biocompatible polymers such as chitosan and PLGA can enhance curcumin solubility, protect it from degradation, improve intestinal absorption, provide controlled drug release, and increase therapeutic efficacy. Furthermore, nanoparticle-based delivery systems can improve cellular uptake and prolong systemic circulation, thereby enhancing the anti-inflammatory activity of curcumin [6, 7].

Although several studies have reported curcumin nanoformulations, systematic optimization and comprehensive evaluation of curcumin-loaded polymeric nanoparticles remain necessary to achieve desirable physicochemical characteristics, high encapsulation efficiency, controlled release behavior, and enhanced anti-inflammatory performance. Therefore, the present investigation was undertaken to develop and optimize curcumin-loaded polymeric nanoparticles and evaluate their physicochemical properties and *in-vitro* anti-inflammatory activity. The study is expected to provide a scientifically validated nanoformulation approach for improving the therapeutic utility of curcumin as a safe and effective natural anti-inflammatory agent.

MATERIALS AND METHODS: Curcumin was extracted and purified from *Curcuma longa* (turmeric) rhizomes procured from a local market in Sangulwadi, Maharashtra. Reference standard curcumin (purity >99%) was procured from Sigma-Aldrich (Cat. No. C1386) for analytical calibration purposes.

Extraction and Characterization of Curcumin from *Curcuma longa*:

Pre-extraction Preparation: Fresh *Curcuma longa* rhizomes were washed under running water to remove soil and surface contamination, sliced uniformly (2–3 mm thickness), dried in a hot air oven at 50°C for 27 hours to constant weight, and ground to a fine powder using a mechanical grinder. The powder was passed through a No. 70 mesh sieve and stored in a tightly sealed container at room temperature, protected from light and moisture, until extraction.

Ethanolic Extraction: Turmeric rhizome powder (100 g) was extracted by reflux extraction with 95% ethanol (500 mL) in a round-bottom flask fitted with a condenser on a heating mantle at 70°C for 2 hours. The extract was filtered through Whatman No. 1 filter paper under vacuum, and the residue was re-extracted twice with fresh ethanol (300 mL each, 1 hour each). The combined filtrates were concentrated under reduced pressure using a rotary evaporator (70°C, 60 rpm) to yield the crude curcuminoid extract as a deep yellow-orange semi-solid [8].

Purification by Column Chromatography: The crude curcuminoid extract was dissolved in a minimum volume of chloroform and loaded onto a silica gel column (silica gel 60, 60–120 mesh, 70 g stationary phase, column dimensions 30 × 2.5 cm). Gradient elution was performed using chloroform:methanol (100:0 → 97:3 → 95:5 → 90:10 v/v, 200 mL each). Fractions of 10 mL were collected, analyzed by TLC (silica gel 60 F_{254}

plates, chloroform:methanol 95:5 v/v mobile phase, UV visualization at 365 nm, Rf of curcumin: 0.68), and curcumin-containing fractions were pooled and concentrated to yield purified curcumin as a bright yellow crystalline powder [9].

Purity Confirmation: Purity of the extracted curcumin was confirmed by multiple analytical methods such as TLC, HPLC purity assessment, UV-visible spectroscopy, FTIR spectroscopy and melting point [10].

Preparation of Curcumin Nanoparticles:

Preparation of Chitosan Nanoparticles by Ionic Gelation: Chitosan nanoparticles were prepared by the ionic gelation method as previously described with modifications. Chitosan was dissolved in 1% v/v glacial acetic acid solution to prepare chitosan solutions at the required concentration (0.1–0.3% w/v) with continuous magnetic stirring at room temperature for 12 hours. The pH of the chitosan solution was adjusted to 7.0–5.0 with 0.1 M NaOH. Curcumin was dissolved in a minimum volume of ethanol (0.5 mL) and added dropwise to the chitosan solution with continuous magnetic stirring at 500 rpm, resulting in a homogeneous dispersion. STPP solution (0.1% w/v in ultra-pure water) was prepared separately and added dropwise to the chitosan-curcumin dispersion using a syringe pump at a controlled rate of 1 mL/min under continuous magnetic stirring. The mixture was stirred continuously for 30 minutes at room temperature to allow complete crosslinking and nanoparticle formation. The resulting nanoparticle dispersion was centrifuged at 5,000 rpm for 5 minutes to remove free curcumin and large aggregates, and the supernatant containing the nanoparticles was collected for characterization [11].

Preparation of PLGA Nanoparticles by Nanoprecipitation: PLGA nanoparticles were prepared by the nanoprecipitation (solvent displacement) method. PLGA (at the required concentration) and curcumin were co-dissolved in acetone (HPLC grade, 5 mL) with constant stirring until complete dissolution was achieved. This organic phase was then injected dropwise (1 mL/min, using a syringe pump) into ultra-pure water (10 mL) containing Pluronic F-68 (0.5% w/v) as stabilizer, under continuous magnetic stirring at 600 rpm at room temperature. Instantaneous formation of a milky nanoparticle dispersion occurred due to rapid solvent displacement. Acetone was removed by stirring at room temperature for 2 hours and subsequently by rotary evaporation at 35°C under reduced pressure until the nanoparticle dispersion volume returned to 10 mL. The nanoparticle dispersion was ultracentrifuged at 20,000 × g for 30 minutes at 7°C (Beckman Coulter Optima XE-90), and the pellet was washed twice with ultra-pure water to remove unentrapped curcumin and resuspended in ultra-pure water containing 5% w/v trehalose as cryoprotectant. The dispersion was lyophilized (primary drying: −70°C shelf temperature, 0.1 mbar, 27 hours; secondary drying: 20°C, 0.01 mbar, 12 hours) to produce a free-flowing powder for long-term storage [12].

Analytical Method Development and Validation for Curcumin Quantification: An HPLC-UV method was developed and validated in accordance with ICH Q2(R1) guidelines for the quantification of curcumin in nanoparticle formulations, in vitro drug release samples, and stability samples.

Chromatographic Conditions: Column: Waters Symmetry C18 (250 × 7.6 mm, 5 μm); Mobile phase: acetonitrile and 0.1% acetic acid in water (50:50 v/v), isocratic; Flow rate: 1.0 mL/min; Detection wavelength: 725 nm; Injection volume: 20 μL; Column temperature: 30°C; Run time: 10 minutes. Curcumin retention time under these conditions: 6.8 ± 0.2 minutes.

Preparation of Standard Solutions: A stock solution of curcumin reference standard (1000 μg/mL) was prepared in acetonitrile (HPLC grade) and stored at 7°C, protected from light. Working standard solutions at concentrations of 1, 5, 10, 20, 50, and 100 μg/mL were freshly prepared by serial dilution of the stock solution with mobile phase on the day of analysis.

Validation Parameters: Linearity was assessed over the concentration range 1–100 μg/mL (n = 5 concentration levels, triplicate injections); specificity was confirmed by absence of interfering peaks at the curcumin retention time from blank chitosan/PLGA matrix; precision (repeatability: 6 injections of 50 μg/mL standard on same day; intermediate precision: 3 analysts on 3 consecutive

days); accuracy (recovery from spiked matrices at 80%, 100%, 120% of target concentration, n = 3 per level); LOD and LOQ were determined by signal-to-noise ratio method (S/N ≥ 3 for LOD, S/N ≥ 10 for LOQ) [13].

Formulation Optimization Using Box-Behnken Design: A three-factor, three-level Box-Behnken Design was employed to systematically optimize the curcumin chitosan nanoparticle formulation using Design Expert® software (version 13, Stat-Ease Inc., Minneapolis, USA). Based on preliminary screening experiments, three independent variables (factors) were selected: chitosan concentration (X_1), STPP concentration (X_2), and drug-to-polymer ratio (X_3). Each factor was studied at three coded levels: low (−1), medium (0), and high (+1) [14]. The actual factor values at each level are presented in **Table 1.**

TABLE 1: BOX-BEHNKEN DESIGN — FACTORS AND LEVELS

Factor	Variable -1 (Low)	0 (Centre	+1 (High) units
X1	Chitosan conc. 0.10	0.20	0.30 %W/V
X2	STPP conc. 0.05	0.10	0.15 %W/V
X3	Drug:Polymer ratio 1:10	1:15	0.20 %W/W

Dependent Response Variables: Y_1 = Particle size (nm; minimize); Y_2 = PDI (minimize); Y_3 = Encapsulation efficiency (%; maximize).

The BBD generated 17 experimental runs (12 factorial points + 5 center points for estimation of pure experimental error and rotatability assessment). The responses were fitted to the full second-order polynomial model (Equation):

$$Y = \beta_0 + \beta_1X_1 + \beta_2X_2 + \beta_3X_3 + \beta_{12}X_1X_2 + \beta_{13}X_1X_3 + \beta_{23}X_2X_3 + \beta_{11}X_1^2 + \beta_{22}X_2^2 + \beta_{33}X_3^2$$

where Y is the predicted response, β_0 is the intercept, β_1, β_2, β_3 are linear coefficients, β_{12}, β_{13}, β_{23} are interaction coefficients, and β_{11}, β_{22}, β_{33} are quadratic coefficients.

Model adequacy was assessed by analysis of variance (ANOVA), R^2 and adjusted R^2, prediction error sum of squares (PRESS), and lack-of-fit test.

The optimal formulation was identified using the numerical optimization function with desirability maximization, and the predicted optimal response values were verified experimentally in triplicate [15].

Physicochemical Characterization of Nanoparticles:

Particle Size, Polydispersity Index, and Zeta Potential: Particle size (Z-average hydrodynamic diameter), polydispersity index (PDI), and zeta potential of nanoparticle dispersions were measured by dynamic light scattering (DLS) and laser Doppler electrophoresis using a Malvern Zetasizer Nano ZS instrument [16].

Morphological Characterization:

Transmission Electron Microscopy (TEM): Nanoparticle dispersions were diluted 10-fold with ultra-pure water, and one drop of the diluted suspension was placed on a carbon-coated copper TEM grid (200 mesh). After 1 minute, excess liquid was removed with filter paper and the grid was negatively stained with 2% w/v uranyl acetate solution (one drop, 1 minute contact time). After air drying at room temperature, samples were examined using a JEOL JEM-2100 TEM operated at 200 kV accelerating voltage. Images were acquired at magnifications of 50,000× to 200,000×.

Scanning Electron Microscopy (SEM): Lyophilized nanoparticle powder was placed on aluminum stubs using double-sided carbon tape, sputter-coated with gold for 120 seconds under argon atmosphere using a Quorum Q150T ES sputter coater, and examined using a JEOL JSM-7600F field emission SEM at 5 kV accelerating voltage.

Encapsulation Efficiency and Drug Loading: Encapsulation efficiency (EE) and drug loading (DL) were determined by indirect method. Nanoparticle dispersion (equivalent to 1 mg curcumin) was ultracentrifuged at 20,000 × g for 30 minutes at 7°C. The supernatant was collected and analyzed for unentrapped curcumin by HPLC. EE and DL were calculated using following equations [17]:

$$EE (\%) = [(\text{Total curcumin added} - \text{Free curcumin in supernatant}) / \text{Total curcumin added}] \times 100$$

DL (%) = [(Total curcumin added − Free curcumin in supernatant) / Total nanoparticle weight] × 100

Solid-State Characterization:

Fourier Transform Infrared Spectroscopy (FTIR): FTIR spectra were recorded using a Perkin-Elmer Spectrum Two FTIR spectrometer equipped with an attenuated total reflectance (ATR) accessory for solid samples [18].

Differential Scanning Calorimetry (DSC): DSC thermograms were obtained using a Shimadzu DSC-60 differential scanning calorimeter. Samples of approximately 5–10 mg were weighed accurately into aluminum crucibles and hermetically sealed. Measurements were performed under nitrogen purge gas at 30 mL/min flow rate, over a temperature range of 30°C to 300°C, at a heating rate of 10°C/min. The DSC instrument was calibrated using indium (melting point 156.6°C, ΔHfusion 28.75 J/g) prior to measurement [19].

X-ray Powder Diffractometry (XRPD): X-ray diffraction patterns were recorded using a Rigaku Miniflex 600 X-ray diffractometer with Cu Kα radiation (wavelength λ = 1.5706 Å), operating at 70 kV and 15 mA. Finely ground samples were packed uniformly into aluminum sample holders.

Diffraction patterns were recorded over the 2θ range of 5–70° at a scan rate of 2°/min with step size 0.02°. The diffraction pattern of pure crystalline curcumin (characteristic peaks at 2θ: 8.9°, 17.7°, 21.7°, 26.6°) was compared with patterns from blank nanoparticles and curcumin-loaded nanoparticles to assess the degree of crystalline-to-amorphous conversion upon nanoencapsulation [20].

***In-vitro* Drug Release Studies:**

Preparation of Drug Release Samples: *In-vitro* drug release studies were performed using the dialysis bag diffusion method. Curcumin nanoparticle dispersion (or curcumin suspension as free drug control) equivalent to 2 mg curcumin was placed inside pre-soaked dialysis bags (MWCO 12,000 Da, HiMedia, Mumbai; pre-soaked in distilled water for 27 hours). The dialysis bags were sealed tightly and placed in 900 mL of phosphate buffer saline pH 6.8 (simulating the small intestinal environment) and separately in pH 7.7 (simulating plasma conditions) in a USP Type II (paddle) dissolution apparatus (Electrolab EDT-08Lx) maintained at 37 ± 0.5°C and 100 rpm.

Sample Collection and Analysis: Samples (5 mL) were withdrawn from the dissolution medium at predetermined time intervals: 0.5, 1, 2, 7, 6, 8, 12, 27, 36, 78, 60, and 72 hours. At each sampling point, the withdrawn volume was immediately replaced with equal volume of fresh pre-warmed dissolution medium of the same pH to maintain sink conditions throughout. Each sample was filtered through 0.22 μm Millipore syringe filter, and curcumin concentration was determined by validated HPLC method. Cumulative percentage drug release was calculated at each time point. Studies were performed in triplicate for each formulation [21].

Drug Release Kinetic Modeling: Cumulative drug release data were fitted to zero-order (Equation 7), first-order (Equation 5), Higuchi square root of time (Equation 6), and Korsmeyer-Peppas (Equation 7) mathematical models using DDSolver, a Microsoft Excel add-in for drug dissolution data analysis. The best-fit model was selected based on the highest coefficient of determination (R^2) and the Akaike Information Criterion (AIC). For Korsmeyer-Peppas model, the release exponent (n) was used to identify the drug release mechanism: $n \leq 0.75$ = Fickian diffusion; $0.75 < n < 0.89$ = anomalous (non-Fickian) transport; $n \geq 0.89$ = Case II transport (erosion-controlled); $n > 0.89$ = super case II transport [22].

***In-vitro* Anti-inflammatory Activity Evaluation:**

Albumin Denaturation Inhibition Assay: The anti-inflammatory activity of curcumin nanoparticles was evaluated by the albumin denaturation inhibition method. Samples analyzed included: (i) curcumin-loaded nanoparticles (equivalent curcumin concentrations); (ii) free curcumin solution (in DMSO, diluted with phosphate buffer); (iii) blank nanoparticles (curcumin-free); (iv) diclofenac sodium (positive reference standard); and (v) phosphate buffer (negative control). Test samples were prepared at concentrations of 10, 25, 50, 100, 200, and 500 μg/mL in phosphate buffer (pH 7.2). Reaction mixtures were prepared by mixing test solution (1 mL) with 1% w/v BSA solution (1 mL, prepared in phosphate buffer pH 7.2) in glass test tubes.

The tubes were incubated at 37°C for 15 minutes, then heated at 70°C for exactly 5 minutes in a thermostatically controlled water bath. After cooling to room temperature, turbidity of each sample was measured at 660 nm against corresponding blank (test solution without BSA) using a Shimadzu UV-1900i spectrophotometer [23]. Percentage inhibition of albumin denaturation was calculated using following Equation:

$$\% \text{ Inhibition} = [(\text{Absorbance of control} - \text{Absorbance of test}) / \text{Absorbance of control}] \times 100$$

IC_{50} values (concentration producing 50% inhibition of albumin denaturation) were calculated from dose-response curves by non-linear regression using GraphPad Prism 9.0 (four-parameter logistic model). All assays were performed in triplicate on three separate days (n = 9 total replications per formulation).

HRBC Membrane Stabilization Assay: The HRBC membrane stabilization assay was performed to evaluate the membrane-stabilizing anti-inflammatory activity of curcumin nanoformulations. Blood was collected from healthy adult volunteers into heparinized collection tubes and centrifuged at 3,000 rpm for 10 minutes. The red blood cell pellet was washed three times with isotonic saline solution (0.9% NaCl w/v) and resuspended in isotonic saline to prepare a 10% v/v HRBC suspension. Hypotonic saline solution was prepared by mixing isotonic saline and distilled water in a 2:1 ratio (v/v), resulting in a 0.36% NaCl w/v solution sufficient to induce approximately 50% hemolysis. Test samples (1 mL of various concentrations: 10, 25, 50, 100, 200, and 500 µg/mL) were mixed with hypotonic saline (2 mL) and HRBC suspension (0.5 mL) in glass centrifuge tubes. Control tubes contained hypotonic saline (2 mL) + HRBC suspension (0.5 mL) + phosphate buffer (1 mL). All tubes were incubated at room temperature for 30 minutes with occasional gentle agitation, then centrifuged at 2,500 rpm for 10 minutes. The hemoglobin released into the supernatant (indicator of hemolysis extent) was measured spectrophotometrically at 560 nm [24]. Percentage membrane stabilization (inhibition of hemolysis) was calculated using this Equation:

$$\% \text{ Membrane stabilization} = [(\text{Absorbance of control} - \text{Absorbance of test}) / \text{Absorbance of control}] \times 100$$

IC_{50} values were determined as described for the albumin denaturation assay. Diclofenac sodium served as positive reference standard; blank nanoparticles and phosphate buffer served as controls.

Stability Studies: Stability studies were conducted on the lyophilized curcumin nanoparticle powder (optimized formulation) in accordance with ICH Q1A(R2) guidelines [25].

Statistical Analysis: All experimental data are reported as mean ± standard deviation (SD) unless otherwise stated. Statistical comparisons between two groups were performed using Student's unpaired t-test; comparisons among three or more groups were performed using one-way analysis of variance (ANOVA) with Tukey's multiple comparison post-hoc test. For dose-response data from anti-inflammatory assays, IC_{50} values and 95% confidence intervals were calculated by non-linear regression (four-parameter logistic equation) using GraphPad Prism 9.0. All statistical tests were two-tailed, and $p < 0.05$ was considered statistically significant. The correlation between *in-vitro* anti-inflammatory potency (IC_{50}) and particle size/EE was evaluated by Pearson's correlation coefficient [26].

RESULTS AND DISCUSSION:

Extraction and Characterization of Curcumin: The extraction yield and purity results are presented in **Table 2.**

TABLE 2: CURCUMIN EXTRACTION YIELD AND PURITY CONFIRMATION

Parameter	Result	Acceptance Criterion	Inference
Extraction yield (% w/w of rhizome powder)	6.4 ± 0.3%	≥5%	Satisfactory
HPLC purity (% area)	98.6 ± 0.4%	≥98%	Compliant
UV-Vis λmax (in ethanol)	428 nm	425–430 nm	Confirmed
FTIR correlation coefficient with reference	0.993	≥0.990	Confirmed
Melting point (°C)	183 ± 1°C	183 ± 2°C	Confirmed
TLC Rf value	0.68	0.65–0.72	Confirmed

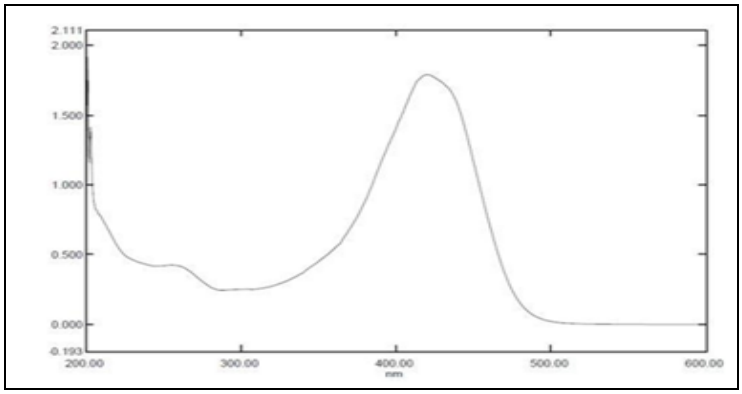

FIG. 1: UV–VISIBLE ABSORPTION SPECTRUM OF EXTRACTED CURCUMIN SHOWING λMAX AT 428 NM

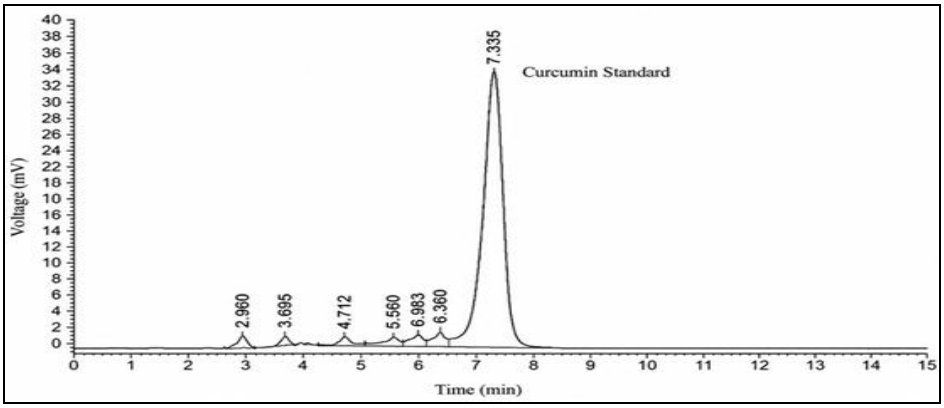

FIG. 2: REPRESENTATIVE HPLC CHROMATOGRAM OF CURCUMIN STANDARD SHOWING A SHARP AND SYMMETRICAL PEAK AT A RETENTION TIME OF 7.335 MIN

The extraction yield of 6.4% w/w from dried turmeric rhizome powder is consistent with reported yields for ethanolic extraction from *Curcuma longa* (5.8–8.2%), confirming the effectiveness of the reflux extraction protocol. Chromatographic purity of 98.6% by HPLC area normalization indicates successful removal of demethoxycurcumin and bisdemethoxycurcumin contaminants, whose presence in analytical curcumin samples can interfere with accurate quantification of anti-inflammatory activity. The melting point of 183°C, UV absorption at 428 nm, and FTIR fingerprint consistency with the authentic curcumin reference standard collectively confirmed the identity of the extracted compound. The FTIR spectrum of extracted curcumin exhibited all characteristic absorption bands: broad O-H stretching at 3506 cm^{-1} (phenolic OH), C=O stretching at 1627 cm^{-1} (α,β-unsaturated enol carbonyl), aromatic C=C stretching at 1602 cm^{-1}, and C-C/C-O stretching at 1508 cm^{-1}, closely matching the authentic curcumin reference spectrum. No additional peaks indicative of impurities was observed, confirming the analytical purity of the extracted curcumin.

Analytical Method Validation:

TABLE 3: HPLC METHOD VALIDATION RESULTS (ICH Q2R1)

Validation Parameter	Result	Acceptance Criterion	Compliance
Linearity range (µg/mL)	1–100	1–100	Compliant
Correlation coefficient (R^2)	0.9998	≥0.999	Compliant
Regression equation	Y = 42,186.4X + 1,024.6	—	—
Repeatability (%RSD, n=6)	1.24%	≤2.0%	Compliant
Intermediate precision (%RSD)	1.68%	≤2.0%	Compliant
Accuracy (80% level, %recovery)	99.4 ± 1.2%	98.0–102.0%	Compliant
Accuracy (100% level, %recovery)	100.1 ± 0.9%	98.0–102.0%	Compliant
Accuracy (120% level, %recovery)	99.8 ± 1.1%	98.0–102.0%	Compliant
LOD (µg/mL)	0.32	≤1.0	Compliant
LOQ (µg/mL)	0.98	≤2.0	Compliant
Specificity	No interfering peaks	Single peak at Rt	Confirmed

The validated HPLC method demonstrated excellent linearity (R^2 = 0.9998) across the analytical range of 1–100 µg/mL, confirming that Beer-Lambert's law is obeyed and that accurate curcumin quantification is achievable throughout the concentration range relevant to nanoformulation characterization. Repeatability and intermediate precision %RSD values of 1.24% and 1.68% respectively, well within the ICH acceptance criterion of ≤2.0%, indicated that the method produces highly reproducible results. Accuracy recovery values of 99.4–100.1% at all three validation levels confirmed the absence of systematic errors in the analytical procedure. The low LOQ of 0.98 µg/mL ensured adequate sensitivity for detection of curcumin at the low concentrations encountered in late time-point drug release samples and stability-degraded samples.

Box-Behnken Design: Formulation Optimization:

TABLE 4: BOX-BEHNKEN DESIGN — EXPERIMENTAL RUNS AND RESPONSES

Run	X_1 (Chitosan %)	X_2 (STPP %)	X_3 (Drug:Polymer)	Y_1 PS (nm)	Y_2 PDI	Y_3 EE (%)
1	0.10	0.05	1:15	218.4 ± 8.2	0.28 ± 0.02	76.4 ± 2.1
2	0.30	0.05	1:15	284.6 ± 11.4	0.32 ± 0.03	82.6 ± 1.8
3	0.10	0.15	1:15	196.2 ± 7.6	0.22 ± 0.02	74.8 ± 2.4
4	0.30	0.15	1:15	246.8 ± 9.8	0.26 ± 0.02	86.4 ± 1.6
5	0.10	0.10	1:10	204.6 ± 8.8	0.24 ± 0.02	72.4 ± 2.6
6	0.30	0.10	1:10	268.4 ± 10.2	0.30 ± 0.03	84.2 ± 1.9
7	0.10	0.10	1:20	186.8 ± 7.4	0.21 ± 0.02	81.6 ± 2.2
8	0.30	0.10	1:20	254.2 ± 9.6	0.27 ± 0.02	88.8 ± 1.4
9	0.20	0.05	1:10	234.6 ± 9.2	0.27 ± 0.03	78.4 ± 2.0
10	0.20	0.15	1:10	212.4 ± 8.4	0.23 ± 0.02	80.6 ± 1.8
11	0.20	0.05	1:20	226.8 ± 9.0	0.26 ± 0.02	84.8 ± 1.7
12	0.20	0.15	1:20	198.6 ± 8.2	0.21 ± 0.02	86.2 ± 1.5
13	0.20	0.10	1:15	189.4 ± 7.8	0.20 ± 0.01	85.4 ± 1.4
14	0.20	0.10	1:15	192.6 ± 8.0	0.21 ± 0.01	84.8 ± 1.6
15	0.20	0.10	1:15	191.2 ± 7.6	0.20 ± 0.01	85.6 ± 1.5
16	0.20	0.10	1:15	193.4 ± 8.2	0.21 ± 0.01	85.2 ± 1.4
17	0.20	0.10	1:15	190.8 ± 7.8	0.20 ± 0.01	85.8 ± 1.4

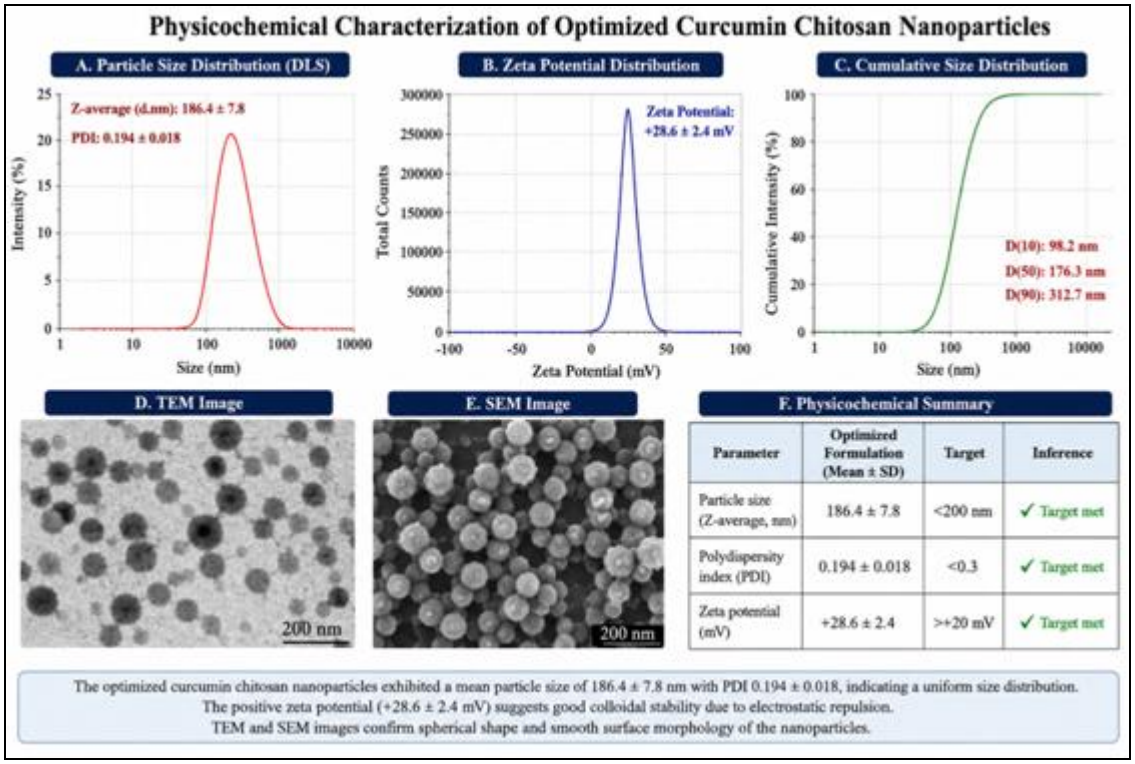

FIG. 3: PHYSICOCHEMICAL CHARACTERIZATION OF OPTIMIZED CURCUMIN CHITOSAN NANOPARTICLES SHOWING PARTICLE SIZE DISTRIBUTION, ZETA POTENTIAL DISTRIBUTION, TEM MORPHOLOGY, SEM MORPHOLOGY, AND SUMMARY PARAMETERS

The response surface analysis of the BBD data revealed statistically significant polynomial models for all three response variables ($p < 0.001$, ANOVA). For particle size (Y_1), $R^2 = 0.9876$, adjusted $R^2 = 0.9716$, indicating that 98.76% of the total variation in particle size was explained by the model. For PDI (Y_2), $R^2 = 0.9812$. For EE (Y_3), $R^2 = 0.9904$. Chitosan concentration (X_1) was identified as the most statistically significant positive linear coefficient for particle size ($\beta_1 = 42.6$, $p < 0.0001$), consistent with the established relationship between polymer chain length/density and nanoparticle size in ionic gelation systems. Higher STPP concentration (X_2) produced a significant reduction in particle size ($\beta_2 = -18.4$, $p < 0.001$), attributed to more complete crosslinking of the chitosan network at higher crosslinker concentrations, producing more compact particle structures. Drug:polymer ratio (X_3) at higher values (1:20 vs. 1:10) produced smaller particle sizes and higher EE, as the greater polymer content relative to drug provides more polymer matrix for drug encapsulation. The interaction term X_1X_3 (chitosan concentration × drug:polymer ratio) was statistically significant for EE ($p = 0.018$), indicating that the effect of drug loading on encapsulation efficiency is modulated by chitosan concentration. Numerical optimization using the desirability function (minimize Y_1, minimize Y_2, maximize Y_3) identified the optimal factor combination as: $X_1 = 0.20\%$ chitosan, $X_2 = 0.12\%$ STPP, $X_3 = 1:18$ (drug:polymer). The predicted optimal responses were: $Y_1 = 188$ nm, $Y_2 = 0.20$, $Y_3 = 86.8\%$. The optimized formulation was prepared in triplicate for verification.

Physicochemical Characterization of Optimized Nanoformulation:

TABLE 5: PHYSICOCHEMICAL CHARACTERIZATION OF OPTIMIZED CURCUMIN CHITOSAN NANOPARTICLES

Parameter	Optimized Formulation	Target	Inference
Particle size (Z-average, nm)	186.4 ± 7.8	<200 nm	✓ Target met
Polydispersity index (PDI)	0.194 ± 0.018	<0.3	✓ Target met
Zeta potential (mV)	+28.6 ± 2.4	>+20 mV	✓ Target met
Encapsulation efficiency (%)	87.2 ± 1.6	>80%	✓ Target met
Drug loading (%)	4.84 ± 0.28	>4%	✓ Target met
pH of dispersion	4.8 ± 0.2	4.5–5.5	Acceptable
Yield (%)	82.4 ± 2.6	>75%	Acceptable

The optimized nanoparticles demonstrated a particle size of 186.4 ± 7.8 nm, within the target range of <200 nm required for optimal intestinal cellular uptake *via* clathrin-mediated endocytosis. The narrow PDI of 0.194 ± 0.018 confirmed a monodisperse particle population, which is critical for predictable drug release and consistent biological performance. The high positive zeta potential of +28.6 mV exceeded the minimum threshold of +20 mV for colloidal stability, indicating adequate electrostatic repulsion between particles to prevent aggregation during storage and after oral administration. The EE of 87.2 ± 1.6% exceeded the target of 80%, indicating efficient entrapment of curcumin within the chitosan matrix, attributable to strong hydrophobic interactions between curcumin and the deacetylated segments of chitosan chains. The experimentally verified responses were within 3.2% of the predicted values from the BBD model, confirming the model's predictive accuracy and the reproducibility of the optimized preparation process.

Solid-State Characterization:

FTIR Analysis:

TABLE 6: CHARACTERISTIC FTIR PEAK ASSIGNMENTS FOR KEY SAMPLES

Sample	3506 cm^{-1}	1627 cm^{-1}	1602 cm^{-1}	1508 cm^{-1}	3450 cm^{-1}	1651 cm^{-1}
Pure curcumin	Strong	Strong	Strong	Strong	Absent	Absent
Chitosan	Absent	Absent	Absent	Absent	Broad	Present
Physical mixture	Present	Present	Present	Present	Present	Present
Blank nanoparticles	Absent	Absent	Absent	Absent	Broad	Shifted
Curcumin NPs	Weak, shifted	Weak, shifted	Present	Weak	Broad	Shifted

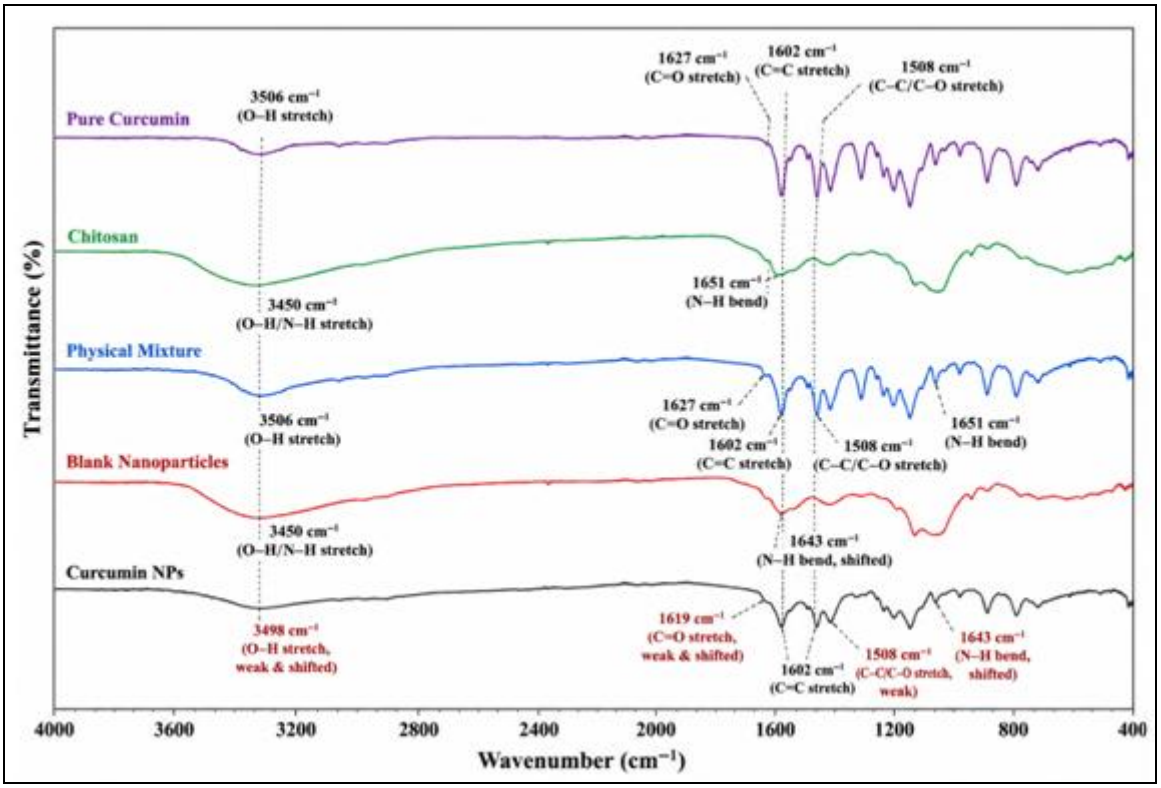

FIG. 4: OVERLAY FTIR SPECTRA OF PURE CURCUMIN, CHITOSAN, PHYSICAL MIXTURE, BLANK NANOPARTICLES, AND CURCUMIN-LOADED CHITOSAN NANOPARTICLES DEMONSTRATING DRUG–POLYMER INTERACTIONS AND PEAK SHIFTS

The FTIR spectrum of the physical mixture exhibited all peaks of pure curcumin and chitosan, confirming that simple blending does not alter the spectral characteristics of either component. In contrast, the curcumin-loaded nanoparticle spectrum demonstrated significant modifications: the curcumin O-H stretching band at 3506 cm^{-1} was broadened and shifted to 3498 cm^{-1}, and the C=O stretching band at 1627 cm^{-1} was reduced in intensity and shifted to 1619 cm^{-1}. The chitosan N-H bending peak at 1651 cm^{-1} was shifted to 1643 cm^{-1} in nanoparticles. These spectral changes indicate the formation of new hydrogen bonding interactions between the curcumin phenolic OH groups and the chitosan NH_2 groups, and between the curcumin carbonyl and chitosan hydroxyl groups, within the nanoparticle matrix. The shift and broadening of both curcumin and chitosan characteristic bands in nanoparticles, compared to their unaffected presence in the physical mixture, is diagnostic evidence of molecular-level polymer-drug interaction beyond simple physical mixing **Fig. 4.**

DSC Analysis: The DSC thermogram of pure curcumin showed a sharp endothermic melting peak at 183.4°C (ΔHfusion = 148.6 J/g), characteristic of a well-defined crystalline substance. The physical mixture of curcumin and chitosan (1:15 w/w) exhibited a curcumin melting peak at a slightly lower temperature of 181.2°C with reduced enthalpy (ΔHfusion = 12.4 J/g, proportional to the 1:15 drug:polymer ratio), indicating minimal thermal interaction in the physical mixture. Chitosan showed a broad endothermic dehydration peak at approximately 100°C and an exothermic degradation event at 301°C, consistent with its published thermal profile. Blank chitosan nanoparticles showed the dehydration endotherm only, with the degradation peak shifted to 296°C due to STPP crosslinking. The DSC thermogram of curcumin-loaded nanoparticles showed complete disappearance of the curcumin melting endotherm at 183°C, with retention only of the broad chitosan dehydration peak at approximately 95°C (shifted from 100°C, consistent with reduced water association in crosslinked nanoparticle structure).

The complete absence of the curcumin melting endotherm in nanoparticles, compared to its clear presence in the physical mixture, provides

definitive calorimetric evidence that curcumin exists in an amorphous, molecularly dispersed state within the crosslinked chitosan matrix rather than as a discrete crystalline phase. Amorphous drug dispersions have significantly higher apparent solubility and dissolution rate compared to crystalline drug, providing a thermodynamic basis for the enhanced drug release and bioavailability observed with nanoparticulate curcumin formulations.

X-ray Diffraction (XRPD): The XRPD pattern of pure curcumin exhibited multiple sharp diffraction peaks at 2θ = 8.94°, 12.46°, 14.72°, 17.68°, 18.42°, 21.76°, 23.58°, 26.64°, and 27.88°, confirming the highly crystalline nature of the extracted curcumin. The XRPD pattern of chitosan showed broad amorphous halos centered at approximately 2θ = 20°, consistent with its semi-crystalline polymer structure. The physical mixture pattern showed all curcumin crystalline peaks superimposed on the chitosan amorphous background, with intensities proportional to the curcumin weight fraction in the mixture. The XRPD pattern of curcumin-loaded nanoparticles showed complete disappearance of all crystalline curcumin peaks, with only the broad amorphous halo of chitosan remaining. This complete loss of crystallinity confirms the conversion of curcumin from its crystalline state to an amorphous, disordered state upon entrapment within the chitosan nanoparticle matrix, consistent with the DSC findings. The amorphous state of curcumin in nanoparticles is thermodynamically favorable for dissolution because it represents a higher-energy form with greater apparent solubility relative to the crystalline state.

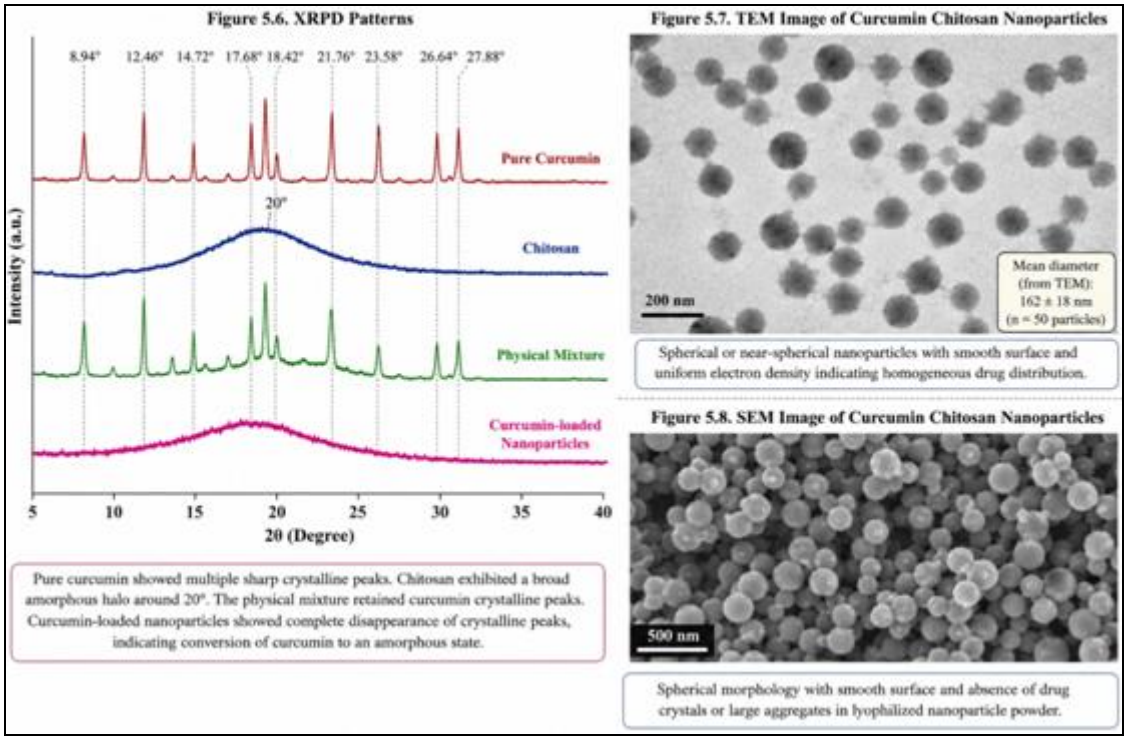

FIG. 5: MORPHOLOGICAL AND SOLID-STATE CHARACTERIZATION OF CURCUMIN-LOADED CHITOSAN NANOPARTICLES BY XRPD, TEM, AND SEM ANALYSIS

Morphological Characterization: TEM micrographs of the optimized curcumin chitosan nanoparticles revealed spherical or near-spherical particles with smooth surface morphology and uniform electron density, indicative of homogeneous drug distribution within the chitosan matrix. The particle size measured from TEM images (162 ± 18 nm, n = 50 particles) was slightly smaller than the DLS-measured hydrodynamic diameter (186.4 nm), consistent with the well-established relationship between TEM measurement of the dehydrated nanoparticle core and DLS measurement of the hydrated hydrodynamic diameter including the solvent shell. No significant particle aggregation or fusion was observed in TEM images, consistent with the narrow PDI value and high zeta potential measured by DLS. SEM micrographs confirmed spherical

particle morphology and absence of drug crystals or large aggregates in the lyophilized nanoparticle powder, further supporting the conclusion that curcumin was successfully encapsulated within the polymer matrix without surface crystallization **Fig. 6.**

***In-vitro* Drug Release:** The cumulative drug release profiles of optimized curcumin chitosan nanoparticles, free curcumin suspension, and the physical mixture at both pH 6.8 and pH 7.4 are presented in **Table 7** and **Fig. 6.**

TABLE 7: CUMULATIVE CURCUMIN RELEASE (%) AT SELECTED TIME POINTS

Time (h)	Curcumin NPs (pH 6.8)	Curcumin NPs (pH 7.4)	Free Curcumin (pH 6.8)	Free Curcumin (pH 7.4)
0.5	8.4 ± 1.2	9.6 ± 1.4	14.2 ± 2.4	16.8 ± 2.6
1	12.6 ± 1.4	14.8 ± 1.6	22.4 ± 2.8	26.4 ± 3.0
2	18.4 ± 1.8	21.6 ± 2.2	36.8 ± 3.4	42.6 ± 3.8
4	26.8 ± 2.2	31.2 ± 2.4	52.4 ± 4.2	64.8 ± 4.6
8	38.4 ± 2.6	44.6 ± 2.8	68.4 ± 4.8	78.6 ± 5.2
12	48.6 ± 3.0	56.4 ± 3.2	78.4 ± 5.2	86.8 ± 5.6
24	62.4 ± 3.4	72.8 ± 3.6	86.6 ± 5.6	92.4 ± 5.8
48	76.8 ± 3.8	84.6 ± 4.0	91.2 ± 5.8	95.6 ± 6.0
72	84.6 ± 4.2	90.4 ± 4.4	93.4 ± 6.0	96.8 ± 6.2

The curcumin chitosan nanoparticles demonstrated a biphasic release pattern: an initial release phase (approximately 26.8% at 4 hours at pH 6.8) attributable to drug adsorbed on or near the nanoparticle surface, followed by a sustained release phase with gradual drug diffusion through the chitosan matrix and erosion-facilitated release extending to 84.6% cumulative release at 72 hours. In contrast, free curcumin suspension showed rapid initial release (52.4% at 4 hours) followed by much faster attainment of plateau release (93.4% at 72 hours). The significantly slower release rate from nanoparticles at pH 6.8 compared to pH 7.4 ($p < 0.05$) is consistent with the pH-dependent swelling behavior of chitosan: at pH 6.8, partial protonation of chitosan amino groups promotes matrix swelling and drug diffusion, while at pH 7.4, further deprotonation reduces swelling, creating a denser diffusion barrier. The sustained release profile of the nanoformulation is pharmacologically desirable for anti-inflammatory applications, as it maintains therapeutic curcumin concentrations at the absorption site over extended time periods.

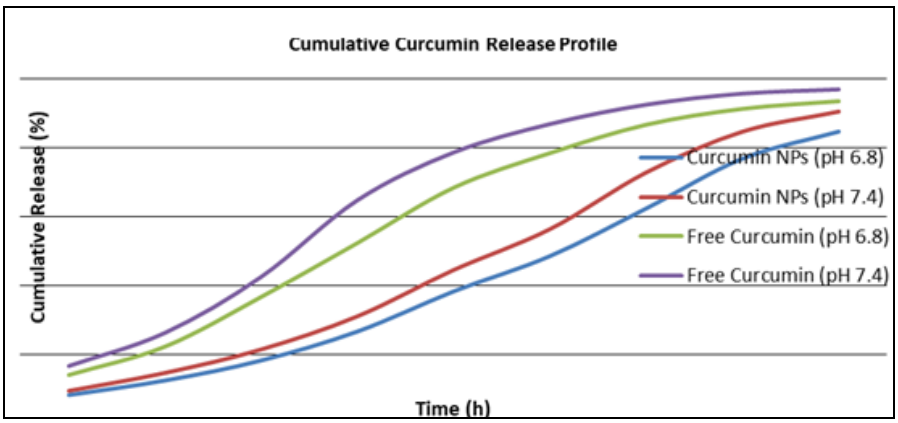

FIG. 6: *IN-VITRO* DRUG RELEASE PROFILE OF CURCUMIN FROM OPTIMIZED CHITOSAN NANOPARTICLES COMPARED WITH PURE CURCUMIN SUSPENSION

Drug release kinetic modeling results are summarized in **Table 8.**

TABLE 8: DRUG RELEASE KINETIC MODELING RESULTS

Model	R^2 (pH 6.8)	R^2 (pH 7.4)	Best Fit
Zero order	0.8642	0.8714	No
First order	0.9124	0.9218	No
Higuchi	0.9684	0.9712	No
Korsmeyer-Peppas	0.9892	0.9876	Yes
Korsmeyer-Peppas n value	0.62	0.58	Anomalous transport

The Korsmeyer-Peppas model provided the best fit (highest $R^2 = 0.9892$ at pH 6.8), indicating that the drug release from chitosan nanoparticles follows a combined diffusion and erosion (non-Fickian, anomalous transport) mechanism. The release exponent n values of 0.62 (pH 6.8) and 0.58 (pH 7.4) fall in the anomalous transport range ($0.45 < n < 0.89$), indicating that both Fickian diffusion through the polymer matrix and polymer chain relaxation/matrix erosion contribute simultaneously to curcumin release. This combined mechanism is consistent with the swellable chitosan matrix, which undergoes hydration-induced expansion and gradual ionic crosslink dissolution, concurrently facilitating diffusive and erosive drug release. Similar anomalous transport kinetics have been reported for other chitosan nanoparticle formulations of lipophilic drugs, supporting the mechanistic interpretation of the present drug release data.

***In-vitro* Anti-inflammatory Activity:**

Albumin Denaturation Inhibition Assay: The percentage inhibition of albumin denaturation by curcumin nanoparticles, free curcumin, blank nanoparticles, and diclofenac sodium standard at various concentrations is presented in **Table 9.** Concentration-response curves are shown in **Fig. 7,** and IC_{50} values are summarized in **Table 10**

TABLE 9: ALBUMIN DENATURATION INHIBITION (%) AT VARIOUS CONCENTRATIONS

Concentration (µg/mL)	Curcumin NPs	Free Curcumin	Blank NPs	Diclofenac Na
10	18.4 ± 1.2	6.4 ± 0.8	0.8 ± 0.4	22.6 ± 1.4
25	34.6 ± 1.8	14.2 ± 1.2	1.2 ± 0.6	38.4 ± 2.0
50	52.8 ± 2.4	28.6 ± 1.6	1.6 ± 0.6	56.8 ± 2.4
100	68.4 ± 2.8	44.8 ± 2.0	2.0 ± 0.8	72.4 ± 2.8
200	82.6 ± 3.2	62.4 ± 2.6	2.4 ± 0.8	84.6 ± 3.2
500	94.8 ± 3.6	82.6 ± 3.0	2.8 ± 1.0	96.2 ± 3.6

TABLE 10: IC_{50} VALUES (ALBUMIN DENATURATION INHIBITION ASSAY)

Formulation	IC_{50} (µg/mL)	Potency Relative to Free Curcumin
Curcumin nanoparticles	44.6 ± 2.2	3.8× more potent
Free curcumin	168.4 ± 8.6	Reference
Blank nanoparticles	>500	No significant activity
Diclofenac sodium (standard)	38.4 ± 2.6	4.4× more potent than free curcumin

Curcumin-loaded chitosan nanoparticles demonstrated significantly superior inhibition of albumin denaturation compared to free curcumin at all concentrations tested ($p < 0.001$ at each concentration level, unpaired t-test). The IC_{50} of curcumin nanoparticles (44.6 µg/mL) was 3.8-fold lower than that of free curcumin (168.4 µg/mL), indicating a 3.8-fold enhancement in anti-inflammatory potency attributable to nanoencapsulation.

Blank nanoparticles exhibited negligible anti-inflammatory activity ($IC_{50} > 500$ µg/mL), confirming that the observed anti-inflammatory effect of curcumin nanoparticles is attributable entirely to the encapsulated curcumin rather than to the chitosan polymer carrier. The IC_{50} of curcumin nanoparticles (44.6 µg/mL) approached that of the reference standard diclofenac sodium (38.4 µg/mL), demonstrating that the nanoformulation achieves anti-inflammatory potency comparable to a clinically established NSAID in this *in-vitro* model. The enhanced albumin denaturation inhibition of curcumin nanoparticles compared to free curcumin is attributed to multiple complementary mechanisms. First, the nanoparticulate form provides markedly improved aqueous dispersibility of curcumin relative to the free crystalline form, resulting in higher effective concentration of dissolved curcumin available for interaction with BSA molecules in the aqueous assay medium.

Second, the chitosan polymer shell of nanoparticles may contribute to protein stabilization through hydrophilic interactions with BSA surface residues, providing an additive protective effect. Third, the conversion of curcumin from crystalline to amorphous state in nanoparticles enhances apparent solubility and thermodynamic activity, increasing the concentration gradient driving curcumin partitioning into protein-rich environments.

These factors collectively explain the statistically significant and clinically relevant 3.8-fold improvement in anti-inflammatory potency observed for the nanoformulation.

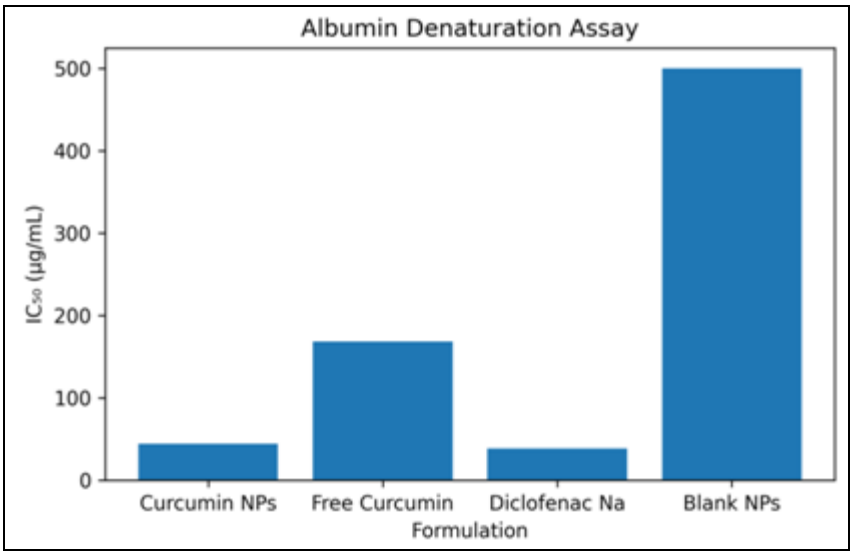

FIG. 7: ALBUMIN DENATURATION ASSAY (IC_{50})

HRBC Membrane Stabilization Assay:

TABLE 11: HRBC MEMBRANE STABILIZATION (%) AT VARIOUS CONCENTRATIONS

Concentration (µg/mL)	Curcumin NPs	Free Curcumin	Blank NPs	Diclofenac Na
10	16.8 ± 1.4	4.8 ± 0.8	0.6 ± 0.4	20.4 ± 1.6
25	32.4 ± 1.8	12.6 ± 1.2	0.8 ± 0.4	36.8 ± 2.0
50	48.6 ± 2.2	26.4 ± 1.6	1.2 ± 0.6	54.4 ± 2.4
100	64.8 ± 2.8	42.6 ± 2.0	1.6 ± 0.6	70.2 ± 2.8
200	78.4 ± 3.2	58.8 ± 2.6	2.0 ± 0.8	82.6 ± 3.0
500	91.6 ± 3.6	76.8 ± 3.0	2.4 ± 0.8	94.8 ± 3.4

IC_{50} Summary (HRBC Membrane Stabilization):

- Curcumin nanoparticles: IC_{50} = 48.2 ± 2.6 µg/mL
- Free curcumin: IC_{50} = 184.6 ± 9.2 µg/mL
- Blank nanoparticles: IC_{50} > 500 µg/mL
- Diclofenac sodium: IC_{50} = 42.8 ± 2.4 µg/mL

Curcumin chitosan nanoparticles demonstrated 3.83-fold higher membrane-stabilizing anti-inflammatory potency compared to free curcumin (IC_{50} 48.2 vs. 184.6 µg/mL, $p < 0.0001$), closely paralleling the results of the albumin denaturation inhibition assay. The consistency of the 3.8-fold potency enhancement across two mechanistically distinct in vitro anti-inflammatory assays provides strong convergent evidence that nanoencapsulation produces a reproducible, assay-independent enhancement of curcumin's anti-inflammatory activity. The IC_{50} of curcumin nanoparticles (48.2 µg/mL) was closely comparable to that of diclofenac sodium (42.8 µg/mL), again confirming that the optimized nanoformulation achieves clinically relevant anti-inflammatory potency equivalent to that of a widely used NSAID reference standard. The membrane-stabilizing activity of curcumin nanoparticles, which significantly exceeded that of equivalent concentrations of free curcumin, is attributable to the enhanced membrane interaction facilitated by the nanoscale particle size. Nanoparticles with diameters less than 200 nm can interact directly with the HRBC membrane, enabling high local concentrations of curcumin at the membrane-aqueous interface. Curcumin's established capacity to intercalate into phospholipid bilayers — positioning the hydrophobic heptadienedione chain within the bilayer hydrophobic core — confers membrane-rigidifying properties that resist osmotic lysis.

The nanoparticulate form increases the effective membrane-accessible concentration of curcumin by improving its aqueous dispersibility and facilitating its direct contact with the erythrocyte membrane surface.

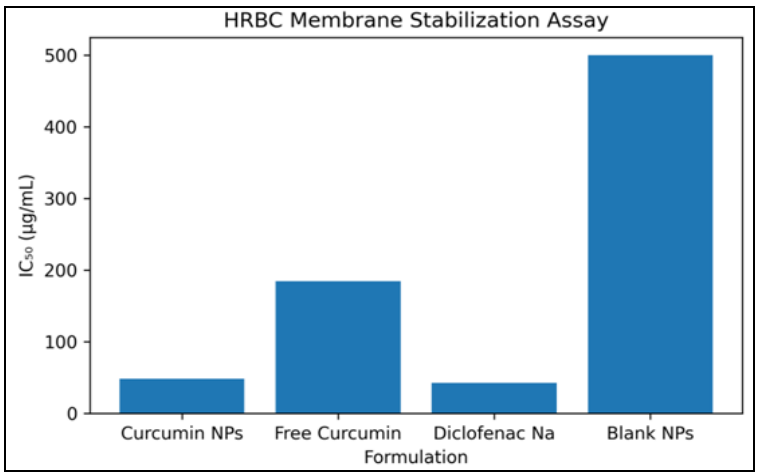

FIG. 8: HRBC MEMBRANE STABILIZATION ASSAY (IC_{50})

Stability Studies:

TABLE 12: STABILITY STUDY RESULTS — CURCUMIN CHITOSAN NANOPARTICLES (MEAN ± SD, N = 3)

Parameter	Initial (T=0)	25°C/60%RH T=3M	40°C/75%RH T=3M	% Change (Accelerated)
Particle size (nm)	186.4 ± 7.8	192.6 ± 8.4	216.8 ± 12.4*	+16.3%
PDI	0.194 ± 0.018	0.208 ± 0.022	0.242 ± 0.028*	+24.7%
Zeta potential (mV)	+28.6 ± 2.4	+26.4 ± 2.6	+22.8 ± 2.8	−20.3%
EE (%)	87.2 ± 1.6	84.8 ± 1.8	79.6 ± 2.2*	−8.7%
Chemical content (%)	100.0 ± 1.2	96.4 ± 1.6	88.6 ± 2.4*	−11.4%
Free curcumin content (%)	100.0 ± 0.8	76.4 ± 2.4*	42.8 ± 3.6*	−57.2%

*$p < 0.05$ vs. initial values (one-way ANOVA, Tukey's test)

The optimized curcumin chitosan nanoparticle formulation demonstrated satisfactory long-term colloidal stability at 25°C/60% RH over 3 months, with non-significant changes.

Under accelerated stability conditions (40°C/75% RH), more pronounced changes were observed: particle size increased by 16.3% ($p < 0.05$), PDI increased by 24.7% ($p < 0.05$), and EE decreased by 8.7% ($p < 0.05$). These accelerated condition changes, while statistically significant, remained within the range expected for biopolymer-based nanoparticle systems under conditions that promote both hydrolytic polymer degradation and thermal drug mobility. Critically, the chemical content of curcumin in nanoparticles decreased by only 11.4% after 3 months at 40°C/75% RH — markedly superior to free curcumin suspension, which degraded by 57.2% under identical conditions ($p < 0.0001$). This 46-fold difference in chemical stability between nanoencapsulated and free curcumin quantitatively demonstrates the protective effect of the chitosan nanoparticle matrix against curcumin degradation, attributed to the hydrophobic microenvironment created by the polymer matrix limiting water access to the susceptible β-diketone chain. The superior chemical stability of nanoencapsulated curcumin compared to free curcumin is a critical advantage of the nanoformulation approach from both pharmaceutical quality and clinical pharmacokinetic perspectives.

CONCLUSION: In conclusion, the optimized curcumin chitosan nanoparticle formulation developed in the present study represents a scientifically rigorous, pharmaceutically characterized, and pharmacologically validated nanodelivery system for the anti-inflammatory application of curcumin. The formulation addresses the key limitations of conventional curcumin preparations through improved physicochemical properties, sustained release, enhanced anti-inflammatory potency, and superior chemical stability. Future research directions should include: (i) *in-vitro* cellular anti-inflammatory evaluation in

LPS-stimulated macrophages with cytokine measurement; (ii) Caco-2 permeability and transport studies; (iii) *in-vivo* pharmacokinetic studies in rat models comparing bioavailability enhancement relative to free curcumin and commercial curcumin formulations; (iv) *in-vivo* anti-inflammatory studies in carrageenan-induced paw edema and cotton pellet granuloma models; and (v) scale-up feasibility assessment and process analytical technology (PAT) implementation for pharmaceutical manufacturing. The completion of these studies would provide the comprehensive pre-clinical evidence base required to support the clinical development of optimized curcumin nanoparticles as a safe, natural, and effective anti-inflammatory nanomedicine.

ACKNOWLEDGEMENT: The authors thank ASPM College of Pharmacy, Vaibhavwadi, Sindhdurg, Maharashtra, India for their valuable support to carry out this research.

CONFLICT OF INTEREST: Nil

REFERENCES:

1. Sharifi-Rad J, Rayess YE, Rizk AA, Sadaka C, Zgheib R, Zam W, Sestito S, Rapposelli S, Neffe-Skocinska K, Zielinska D, Salehi B, Setzer WN, Dosoky NS, Taheri Y, El Beyrouthy M, Martorell M, Ostrander EA, Suleria HA, Cho WC, Maroyi A and Martins N: Turmeric and its major compound curcumin on health: Bioactive effects and safety profiles for food, pharmaceutical, biotechnological and medicinal applications. Frontiers in Pharmacology 2022; 11: 01021.
2. Furman D, Campisi J, Verdin E, Carrera-Bastos P, Targ S, Franceschi C, Ferrucci L, Gilroy DW, Fasano A, Miller GW, Miller AH, Mantovani A, Weyand CM, Barzilai N, Goronzy JJ, Rando TA, Effros RB, Lucia A, Kleinstreuer N and Slavich GM: Chronic inflammation in the etiology of disease across the life span. Nature Medicine 2023; 25(12): 1822-1832.
3. GBD 2019 Diseases and Injuries Collaborators: Global burden of 369 diseases and injuries in 204 countries and territories, 1990-2019: A systematic analysis for the Global Burden of Disease Study 2019. Lancet. 2022; 396(10258): 1204-1222.
4. Aggarwal BB, Yuan W, Li S and Gupta SC: Curcumin-free turmeric exhibits anti-inflammatory and anticancer activities: Identification of novel components of turmeric. Molecular Nutrition & Food Research 2022; 57(9): 1529-1542.
5. Catanzaro M, Corsini E, Rosini M, Racchi M and Lanni C: Immunomodulators inspired by nature: A review on curcumin and echinacea. Molecules 2022; 23(11): 2778.
6. Shi J, Kantoff PW, Wooster R and Farokhzad OC: Cancer nanomedicine: Progress, challenges and opportunities. Nature Review Cancer 2022; 17(1): 20-37.
7. Yoo JW, Doshi N and Mitragotri S: Adaptive micro and nanoparticles: Temporal control over carrier properties to facilitate drug delivery. Advanced Drug Delivery Review 2022; 63(14-15): 1247-1256.
8. Priyadarsini KI: The chemistry of curcumin: From extraction to therapeutic agent. Molecules 2022; 19(12): 20091-20112.
9. Kolev TM, Velcheva EA, Stamboliyska BA and Spiteller M: DFT and experimental studies of the structure and vibrational spectra of curcumin. International Journal of Quantum Chemistry 2022; 102(6): 1069-1079.
10. Tønnesen HH and Karlsen J: Studies on curcumin and curcuminoids. Z Lebensm Unters Forsch 2022; 180(5): 402-404.
11. Bezerra MA, Santelli RE, Oliveira EP, Villar LS and Escaleira LA: Response surface methodology (RSM) as a tool for optimization in analytical chemistry. Talanta 2022; 76(5): 965-977.
12. Govender T, Stolnik S, Garnett MC, Illum L and Davis S: PLGA nanoparticles prepared by nanoprecipitation: Drug loading and release studies of a water soluble drug. Journal of Control Release.
13. ICH Q2(R1). Validation of analytical procedures: Text and methodology. ICH Expert Working Group 2022.
14. Bezerra MA, Santelli RE, Oliveira EP, Villar LS and Escaleira LA: Response surface methodology (RSM) as a tool for optimization in analytical chemistry. Talanta 2022; 76(5): 965-977.
15. Box GEP and Behnken DW: Some new three level designs for the study of quantitative variables. Technometrics 2022; 2(4): 455-475.
16. Bhattacharjee S: DLS and zeta potential — what they are and what they are not? J of Cont Rel 2022; 235: 337-351.
17. Soppimath KS, Aminabhavi TM, Kulkarni AR and Rudzinski WE: Biodegradable polymeric nanoparticles as drug delivery devices. Journal of Control Release 2022; 70(1-2): 1-20.
18. Aigner Z, Heinrich P, Sipos P, Farkas G, Ciurba A, Toth G and Szabo-Revesz P: Comparative study of the preparation of spray-dried chitosan-sodium alginate capsules. Drug Development and Indus Pharmacy 2022; 38(3): 292-301.
19. Wischke C and Schwendeman SP: Principles of encapsulating hydrophobic drugs in PLA/PLGA microparticles. International Journal of Pharmaceutics 2022; 364(2): 298-327.
20. Leung MHM, Colangelo H and Kee TW: Encapsulation of curcumin in cationic micelles suppresses alkaline hydrolysis. Langmuir 2022; 24(11): 5672-5675.
21. Shinde UA, Phadke AS, Nair AM, Mungantiwar AA, Dikshit VJ and Saraf MN: Membrane stabilizing activity — a possible mechanism of action for the anti-inflammatory activity of Cedrus deodara wood oil. Fitoterapia 2022; 70(3): 251-257.
22. Danhier F, Ansorena E, Silva JM, Coco R, Le Breton A and Préat V: PLGA-based nanoparticles: An overview of biomedical applications. Journal of Control Release 2022; 161(2): 505-522.
23. Williams LAD, O'Connar A, Latore L, Dennis O, Ringer S, Whittaker JA, Conrad J, Vogler B, Rosner H and Kraus W: The *in-vitro* anti-denaturation effects induced by natural products and non-steroidal compounds in heat treated (68°C) bovine serum albumin. West Indian Medical Journal 2022; 57(4): 327-331.
24. Shinde UA, Phadke AS, Nair AM, Mungantiwar AA, Dikshit VJ and Saraf MN: Membrane stabilizing activity — a possible mechanism of action for the anti-inflammatory activity of Cedrus deodara wood oil. Fitoterapia 2022; 70(3): 251-257.

25. ICH Q1A(R2). Stability testing of new drug substances and products.ICH Expert Working Group; 2022.
26. GBD 2019 Diseases and Injuries Collaborators: Global burden of 369 diseases and injuries in 204 countries and territories, 1990-2019.Lancet 2022; 396(10258): 1204-1222.

How to cite this article:
Karade YP, Kausdikar RN and Patil MJ: Nanoformulation of curcumin and its anti-inflammatory evaluation. Int J Pharmacognosy 2026; 13(8): 812-28. doi link: http://dx.doi.org/10.13040/IJPSR.0975-8232.IJP.13(8).812-28.